Development of BOLD-sensitive protocols for imaging the human spinal cord at 7 Tesla

Robert L Barry[1,2], John C Gore[1,2], and Seth A Smith[1,2]

[1]*Vanderbilt University Institute of Imaging Science, Nashville, TN, United States,* [2]*Department of Radiology and Radiological Sciences, Vanderbilt University Medical Center, Nashville, TN, United States*

Introduction

Functional magnetic resonance imaging (fMRI) of the human spinal cord was first demonstrated by Yoshizawa et al. [1] in 1996, and has since been demonstrated by a handful of groups worldwide (e.g., [2-9]). Spinal fMRI has been used to study motor and sensory function in the healthy human spinal cord as well as in spinal cord injury (SCI) and multiple sclerosis (MS). With respect to SCI, fMRI has been shown to be sensitive to changes in spinal cord function [10-12]. The majority of spinal injuries are incomplete and loss of function may eventually return to near-normal levels, so spinal fMRI offers a valuable tool for characterizing changes in function due to spontaneous repair and/or surgical intervention. Similarly, in MS, several studies have shows differences in spinal fMRI between MS patients and controls [13-17]. These studies reported regions of activation from C5-C7 with greater signal changes and shifting location in MS patients compared to controls. The most recent study [17] reported activation differences between primary and secondary progressive MS, demonstrating that spinal fMRI can detect differences between patients with MS and controls as well as patient cohorts with various neurological deficits. The majority of spinal fMRI studies have been performed at 1.5 T, and a few have been conducted at 3 T. To date *there have been no reports of human spinal fMRI at any field strength above 3 T*. We are therefore developing novel T_2^*-weighted multi-shot gradient-echo sequences for human 7 T spinal fMRI that achieve high spatial and relatively high temporal resolution, spatial coverage of three or more vertebrae, and minimal geometric distortions. The proposed acquisition and post-processing methods are designed to obviate or mitigate challenges of ultra-high-field fMRI that include tissue heating (specific absorption rate; SAR), T_2^* blurring, and geometric distortions due to static and dynamic magnetic field inhomogeneities.

Methods

Experiments were performed on a Philips Achieva 7 T scanner with a custom-designed 16-channel coil for 7 T cervical spinal imaging (Nova Medical Inc.). Healthy volunteers were scanned under a protocol approved by the institutional review board. Resting state blood oxygenation level dependent (BOLD) data were acquired with a 3D fast field echo (FFE) [18,19] sequence: in-plane field of view = 160 x 160 mm, slice thickness = 4 mm, voxel size = 0.91 x 0.91 x 4 mm^3 (3.31 mm^3), 12 slices, repetition time = 18 ms, echo time (TE) = 7.8 ms, flip angle = 12°, echo train length = 9, sensitivity encoding [20] reduction factor = 1.56 (anterior-posterior), volume acquisition time = 3.49 seconds (291 ms/slice), number of volumes (after 10 dummy scans) = 100, max gradient = 33 mT/m and max slew = 166 T/m/s.

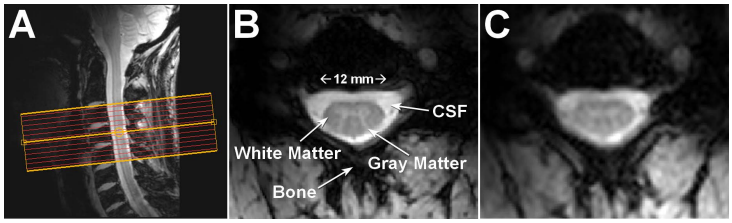

FIG. 1: (**A**) Mid-sagittal slice from a healthy volunteer showing the cervical spinal cord and placement of 12 4-mm thick axial slices covering C3 to C5. (**B**) High-resolution T_2^*-weighted anatomical image at C5 acquired with 0.60 x 0.60 x 4 mm^3 voxels and interpolated to 0.31 x 0.31 x 4 mm^3. Excellent conspicuity permits visualization of the characteristic butterfly-shaped gray matter column. (**C**) A high-resolution functional image of the same slice interpolated to the final resolution of the anatomical. This T_2^*-weighted sequence acquired 12 slices with 0.91 x 0.91 x 4 mm^3 voxels every 3.49 seconds (291 ms/slice). Functional images are high quality with minimal geometric distortions and T_2^* blurring, and facilitate reliable spatial delineation between gray matter, white matter, and cerebrospinal fluid.

Physiological noise correction via RETROICOR [21] (implemented using AFNI [22]) was first applied to each functional run. Co-registration between anatomic and functional data was performed using a 2D Gaussian weighting function applied over the center of the spinal cord in each slice. BOLD images were then warped to the anatomical (`3dAllineate` [22]) using this weighting function and five degrees of freedom (in-plane translation, scaling, and sheering). The quality of resultant transformations was visually verified using MRIcron (www.mccauslandcenter.sc.edu/mricro/mricron). Binary masks identified gray matter, white matter, and cerebrospinal fluid (CSF) for each slice. To further reduce extraneous temporal variance due to physiological noise, principal component analysis was performed on all CSF voxels within each slice to identify slice-specific structured noise sources that may also contaminate gray matter. Principal components that accounted for at least 50% of the cumulative variance in CSF (1-3 components per slice) were used as gray matter 'regressors of no interest' (similar to [23]). Finally, temporal signal-to-noise ratio (TSNR) was calculated across interpolated gray matter voxels (mean divided by standard deviation) as a metric of overall fMRI data quality.

Results

Figure 1 presents data from a healthy volunteer. The mid-sagittal slice shows excellent contrast between the spinal cord and surrounding CSF. Axial slices are planned perpendicular to the cord and obtain coverage of three vertebrae (C3 to C5). High-resolution T_2^*-weighted axial images show the characteristic gray matter butterfly. Our use of multi-shot FFE sequences with short TE and echo trains produce high quality T_2^*-weighted images with minimal T_2^* blurring and geometric distortions. A high degree of geometric fidelity facilitates registration between functional and anatomical images and accurate gray matter segmentation. Spatial plots of TSNR (Fig. 2) reveal mean/median values of 30 across all slices with highest TSNR (up to 50) reported in the ventral horns.

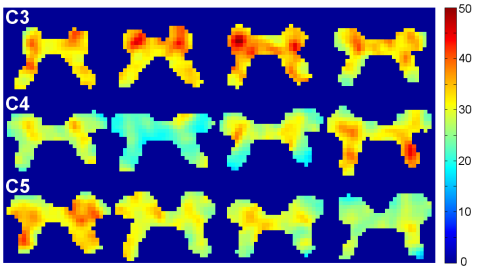

FIG. 2: Temporal signal-to-noise ratio (TSNR) in spinal gray matter within each 4-mm axial slice. Median/mean TSNR=30 and maximum TSNR=50. Results are within the range of published values for cortical gray matter with ~3.3 mm^3 voxels at 7 T [24].

Discussion

To the best of our knowledge, this abstract is the first published demonstration of human spinal fMRI at 7 T. Some of the well-known challenges of 7 T fMRI include T_2^* blurring, geometric distortions, and SAR. The need for high-resolution images with minimal T_2^* blurring and geometric distortions prevent the use of traditional single-shot echo-planar imaging, and both radiofrequency (B_1) inhomogeneities and SAR guidelines prevent effective use of spin-echo based acquisition sequences. Thus, the 3D FFE sequence (with low flip angles and short echo trains) is preferred for the current application. Resultant TSNR are within the range of published values for cortical gray matter with ~3.3 mm^3 voxels at 7 T [24], which suggest that overall signal stability is high and adequate for the current application. Our ongoing work includes continual refinement of the functional protocol and post-acquisition methods, quantification of BOLD signal changes induced by task-based paradigms, and analyses of low-frequency functional connectivity in spinal gray matter. Future work will use the developed methods to investigate and characterize differences in spinal gray matter function and connectivity between healthy controls and cohorts of SCI and MS patients at 7 T.

Acknowledgments – This research was supported by NIH grants 5R01EB000461 and 5K01EB009120.

References – [**1**] Yoshizawa et al. Neuroimage 1996;4:174. [**2**] Stroman et al. MRM 1999;42:571. [**3**] Madi et al. AJNR 2001;22:1768. [**4**] Backes et al. AJNR 2001;22:1854. [**5**] Moffitt et al. JMRI 2005; 21:527. [**6**] Maieron et al. J Neurosci 2007;27:4182. [**7**] Agosta et al. HBM 2009;30:340. [**8**] Cohen-Adad et al. Neuroimage 2010;50:1074. [**9**] Brooks et al. J Neurosci 2012;32:6231. [**10**] Stroman et al. Neuroimage 2002;17:1854. [**11**] Stroman et al. Spinal Cord 42:59. [**12**] Kornelsen & Stroman. Spinal Cord 2007;45:485. [**13**] Agosta et al. Neuroimage 2008;39:1542. [**14**] Agosta et al. MRM 2008;59:1035. [**15**] Agosta et al. Radiology 2009;253:209. [**16**] Valsasina et al. J Neurol Neurosurg Psychiatry 2010;81:405. [**17**] Valsasina et al. HBM 2012;33:2072. [**18**] van der Meulen et al. MRI 1988;6:355. [**19**] Barry et al. Neuroimage 2011;55:1034. [**20**] Pruessmann et al. MRM 1999;42:952. [**21**] Glover et al. MRM 2000;44:162. [**22**] Cox. Comput Biomed Res 1996;29:162. [**23**] Xie et al. Neuroimage 2012;63:245. [**24**] Triantafyllou et al. Neuroimage 2005;26:243.